



Modeling and performance evaluation of an electromechanical valve actuator for a camless IC engine

Eid Mohamed

Automotive and Tractors Engineering, Faculty of Engineering, Helwan University, Cairo, Egypt.

Abstract

Valve train control is one of the best strategies for optimizing efficiency and emissions of Internal Combustion (IC) engines. Applications of solenoid valve actuators in (IC) engines can facilitate operations such as variable valve timing and variable valve lifting for improved the engine performance, fuel economy and reduce emission, the electromechanical valve actuator (EMVA) uses solenoid to actuate valve movement independently for the application of (IC) engine. In this work presents the effects of design and operating parameters on the system dynamic performances of the actuator and the proposed an (EMVA) structure by incorporating the hybrid magneto-motive force (MMF) implementation in which the magnetic flux is combined by the coil excitation and permanent magnets.

A two-degree-of-freedom lumped parameter model is used to simulate the response of valve actuator system in the opening and closing. The model and control of an electromagnetic valve (EMV) are described. This is done using electromagnetic force to open and close the valve and a controller regulates the motion specifications required. The developments controller is based on a state-space description of the actuator that is derived based on physical principles and parameter identification. Linear-quadratic regulator design (LQR) optimal control is designed with the evaluation reasonable the performance and energy of (EMV) valve are obtained with the design.

Copyright © 2012 International Energy and Environment Foundation - All rights reserved.

Keywords: Electromagnetic solenoid actuator; Magnetic flux; Actuator design; Variable valve timing; Engine fuel economy.

1. Introduction

In recent years camless engine has caught much attention in the automotive industry. Camless valve train offers programmable valve motion control capability. However, it also introduces valve train control issues. There are mainly two types of electromechanically actuators; electro-hydraulic valve. Variable valve actuation (VVA) is an existing method that offers enhanced potential for improving the automotive internal combustion engine. The electromagnetic valve drive system EMVD apparatus was designed, constructed, and integrated into a computer-controlled experimental test stand. The experimental results confirm the benefits of using a nonlinear mechanical transformer in a motor driven engine-valve spring system, as seen in the small average power consumption and low valve seating velocity. In addition, a valve transition time sufficient for 6000-rpm engine operation was achieved. The results also suggest ways to improve the EMVD apparatus in the future. Originally, this concept of independent valve control was patented in [1, 2] with the rationale of increasing engine torque over a wide range of speed and load conditions. As legislation on fuel economy and emissions become increasingly stringent, the emphasis on

torque improvements gradually shifted towards cleaner burning and ancient engines. Many modern automobile engines operate with devices that either performs a camshaft phase shift varying only valve timing to offer engine performance improvements at certain engine operating points. These "camshaft add-on" devices are reliable, however, their ability to provide valve timing variations are fractional when compared to a system that possess full VVA capabilities. Valve actuation by electromagnets can provide control flexibility over an engine valve phase, either independently or simultaneously with other valves. Having such flexibility in valve variation are advantages:

1. Increase maximum power at high speed: If closing of the intake valve is delayed under high engine loads, the significant air-fuel momentum in the intake means that even after the piston starts moving up, fresh air continues entering the combustion chamber instead of being pushed out. The result is better compression and more power.
2. Improve engine efficiency at low speed: When the engine is under partial load, the intake valve would be closed early to reduce the suction force needed to bring the air in (pumping loss). In addition, because less air needs to be compressed, the engine generates less heat, and thus, the thermal efficiency is improved. These efficiency improvements translate into less fuel consumption at low engine loads.
3. Reduce pollution using Exhaust Gas Recirculation (EGR): Traditionally, in order to reduce nitrogen-oxide (NO_x) emissions generated from engines operating at high temperatures, EGR valves are placed in the engine to reduce the combustion temperature by recycling the exhaust back into the intake valve. Variable valve actuation can remove the need for additional valves by regulating the overlaps between intake and exhaust valve openings or by closing the exhaust valve early.

The analysis of the upper electromagnet has been performed using finite element (FEM) simulation; thereby an axially symmetrical 2D. FEM model in COMSOL Multiphysics has been used taking into account all nonlinear effects. The calculated static characteristics are implemented in a SIMULINK model to simulate the dynamics of the EMVA [3].

The electromechanical valve train (EMV) technology allows for a reduction in fuel consumption while operating under a stoichiometric air-fuel-ratio and preserves the ability to use conventional exhaust gas after treatment technology with a three- way-catalyst. Compared with an engine with a camshaft-driven valve train, the variable valve timing concept makes possible an additional optimization of cold start, warm-up and transient operation. In contrast with the conventionally throttled engine, optimized control of load and in-cylinder gas movement can be used for each individual cylinder and engine cycle. A load control strategy using a "Late Intake Valve Open"(LIO) provides a reduction in start-up HC emissions of approximately 60%. Due to reduced wall-wetting, the LIO control strategy improves the transition from start to idle. "Late Exhaust Valve Open"(LEO) timing during the exhaust stroke leads to exhaust gas afterburning and, thereby, results in high exhaust gas temperatures and low HC emissions. Vehicle investigations have demonstrated an improved accuracy of the air-fuel-ratio during transient operation. Results in the New European Driving Cycle have confirmed a reduction in fuel consumption of more than 15% while meeting EURO IV emission limits [4].

The flux linkage model was assumed to have two regions, a linear region and a saturation region. Different model formats were constructed for different regions, yet only the linear region model was used for control design in later stage. Model parameters were identified for both regions with the directly measurement of electromagnetic force and valve lift, A dual flux channels EMVA is detailed and the design procedures are presented. Comparing with the conventional EMV, the proposed prototype shows a lot of advantages such as compactness, high temperature tolerance, fast response, relieve of starting current, and variable current actuating timing. The nonlinear controller based on Sontag's feedback to render the electromechanical valve actuator (EVA) globally asymptotically stable (GAS). Electromechanical valve actuators have received much attention recently due to their potential for improving the performance of the internal combustion engine [5, 6].

2. Principle of electromechanical valve actuator

A typical construction of EMV consists of two magnets (closer and opener), two springs (an actuator and a valve spring) and a moving armature that is connected to an engine valve. Normally, most modern engines incorporate a hydraulic lash adjuster to ensure proper valve sealing under all thermal operating conditions. The current flowing in the coil creates a magnetic force on the armature to overcome compressive spring and friction forces. Both springs are adjusted such that they are always in

compression for any armature position between the two electromagnets. Preloading these springs are ideal for achieving rapid flight time and minimizing electrical energy input. During normal operation, the spring forces are utilized to accelerate the moving masses while electromagnetic forces are utilized to attract and dwell the armature.

Figure 1 illustrates a typical operational mode of the EMV actuator. To move the valve from neutral to closed position, a routine is initialized to impart sufficient armature momentum for the closer coil magnetic forces to attract the armature. Once contact is established and quasi-static conditions are reached, a holding current is applied to the upper coil so that sufficient magnetic force is generated to overcome spring forces while holding the armature and valve in the fully closed position. When the valve is commanded to open, the upper coil current is rapidly discharged, allowing magnetic force to decay and the actuator spring to push the armature down. The lower coil is then activated to capture the approaching armature. The electromagnetic force generated is proportional to the volume of the electromagnet. The design volume of the electromagnet is limited by the area in the cylinder head. Thus a compromise has to be made in the design and operation of an engine using EMV system. This compromise is usually in the form of a limited volumetric efficiency and maximum operating speed of the engine [7, 8].

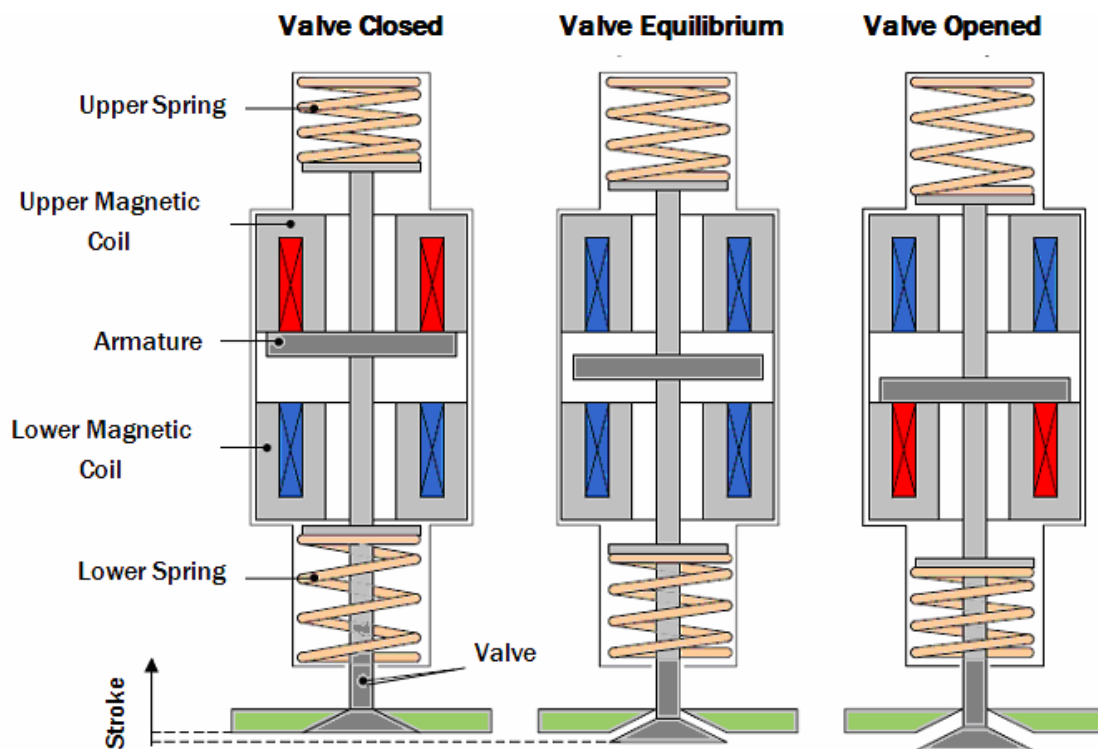


Figure 1. shows a schematic of an EMV actuator mounted on a cylinder head

3. Kinetics of EMV actuator

3.1 Current to magnetic force model

Magnetic circuits of EMV, Ref. [9] considers that characterize the behavior of the magnetic fields within a given device or set of devices, can be analyzed using the circuit analysis techniques defined for electric circuits.

The quantities of interest in a magnetic circuit are the vector magnetic field H , the vector magnetic flux density B_f and the total magnetic flux λ_m . The vector magnetic field and vector magnetic flux density are related by:

$$B_f = \mu H = \mu_r \mu_o H \quad (1)$$

Where

μ is the total permeability, μ_r is relative permeability, μ_o is permeability in free space.

There are certain magnetic materials with very high relative permeability's that are commonly found in components of energy systems. These materials (iron, steel, nickel, cobalt, etc.), designated as ferromagnetic materials, are characterized by significant magnetization. Ferromagnetic materials can be thought of as efficient conductors of magnetic fields. The relative permeability's of ferromagnetic materials can range from a few hundred to a few thousand. Ferromagnetic materials are highly nonlinear. That is, the relative permeability is not a constant, but depends on the magnitude of the magnetic field for a given problem. Thus, the relationship between the magnetic field and the magnetic flux density in a nonlinear medium can be written as:

$$B_f = B_s * a \sinh(h_s H) \tag{2}$$

The valve velocity and acceleration is defined as:

$$\frac{dx}{dt} = v \quad \frac{dv}{dt} = a \tag{3}$$

The current- magnetic force relationship is governed by the following equation before magnetic saturation occurs [10, 11]:

$$F_m(x, i) = \frac{K_{ka} i^2}{(K_{kb} + x)^2} \tag{4}$$

$$\frac{di}{dt} = \frac{V_{app} - Ri + Z_1(i, x)v}{Z_2(x)} \tag{5}$$

where $Z_1 = \frac{2K_{ka}i}{(K_{kb} + x)^2}$ and $Z_2 = \frac{2K_{ka}}{(K_{kb} + x)}$, x is the armature displacement, i is the system current, R is the coil resistance, V_{app} is the voltage applied, and k_{ka} and k_{kb} are constants.

Eqns. (2) and (3) neglect the effects of the flux saturation and leakage. When the effect of flux saturation and leakage in magnetic circuit, the magnetic force nonlinear (roughly proportional to inverse distance squared), the effect of magnetic flux saturation and eddy current must be accounted. Figure 2 equivalent electrical circuit of (EMV) system.

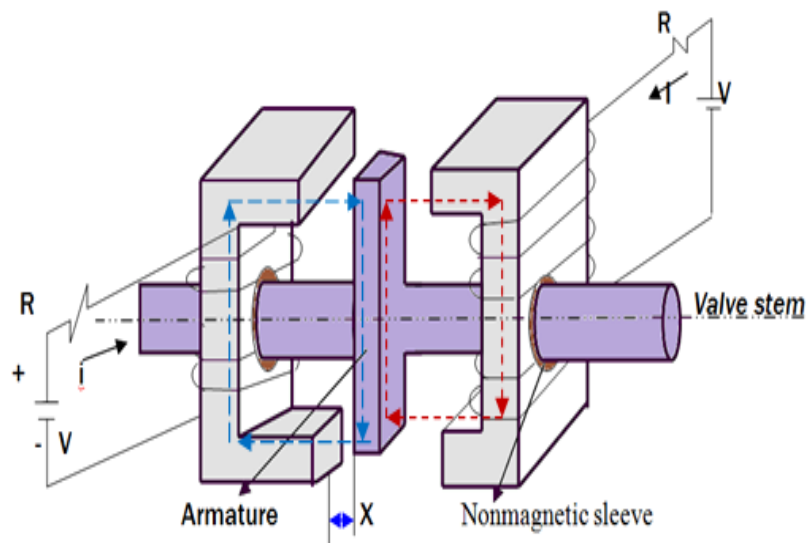


Figure 2. Equivalent circuit diagram of the electrical coil (EMV) subsystem

The following function characterizes the current, i , to magnetic flux, $\lambda(x, i)$ relationship:

$$V = Ri + \frac{d\lambda(x, i)}{dt} \quad (6)$$

$$\lambda = N\phi = N(\phi_l + \phi_m) \quad (7)$$

where $\phi_l = \frac{Ni}{R_l}$ and $\phi_m = \frac{Ni}{R_m}$ are leakage and magnetizing flux, for high dynamic control performance, nonlinearities of flux linkage, $\lambda(x, i)$, are taken into account, namely the saturation of the magnetic circuit. This characteristic is described by a flux linkage-current function:

$$\lambda(x, i) = \lambda_s (1 - e^{-f(x)}) \quad i \geq 0 \quad (8)$$

Where λ_s is the maximum saturated flux, and the function, $f(x) = 2c_1 / (c_2 - x) + c_3$, and c_1, c_2, c_3 constant parameters. The induced EMF opposes the generator voltage polarity. Therefore the generator must do work to push charges through the inductor coil. This work is stored as energy in the magnetic field. Similar to the way energy can be stored in an electric field.

$$E = \int_0^i \lambda(i, x) di = \frac{1}{2\mu_o} B_f^2 AL \quad (9)$$

and the inductance (L) can be expressed as;

$$L = \frac{\lambda}{i} = \frac{N(\phi_l + \phi_m)}{i} \quad (10)$$

The derivative of the co-energy with respect to distance is the magnetic force. The final expression of the magnetic force is derived by substituting in the flux equation;

$$F_m(x, i) = \frac{\lambda_s f'(x)}{f^2(x)} \left[1 - (1 + i(x))e^{-f(x)} \right] \quad (11)$$

The armature movement leads to a reduction of the air gap between the magnets and the armature thereby increasing the magnet efficiency. This is based on the fact that the magnetic force increases in square relation to the air gap for a given current [12, 13].

3.2 Equilibrium of force acting on EMV

The actuating forces on the valve armature are the magnetic, spring, inertia and frictional forces, in addition to the gas pressure force from the engine cylinder, the magnet force is applied to the valve directly through the armature. When no magnetic force exists, the armature is held by the upper and the lower spring in the middle position between the two magnets. This condition occurs when the engine is shut off. During engine operation, a current in the coil of the upper magnet is used to hold the armature against the upper magnet so that the valve is in the close position (equilibrium). To open the valve, the current is interrupted and the armature is moved by the spring-forces to the lower magnet. By providing a current to the coil of the lower magnet, the losses during the movement are compensated and the valve is held in the open position. To close the valve, the current is interrupted in the lower magnet and the current is re-applied to the coil of the upper magnet.

Referring to Figure 3 the equilibrium forces during valve open and close of the EMV releasing dynamics are described by:

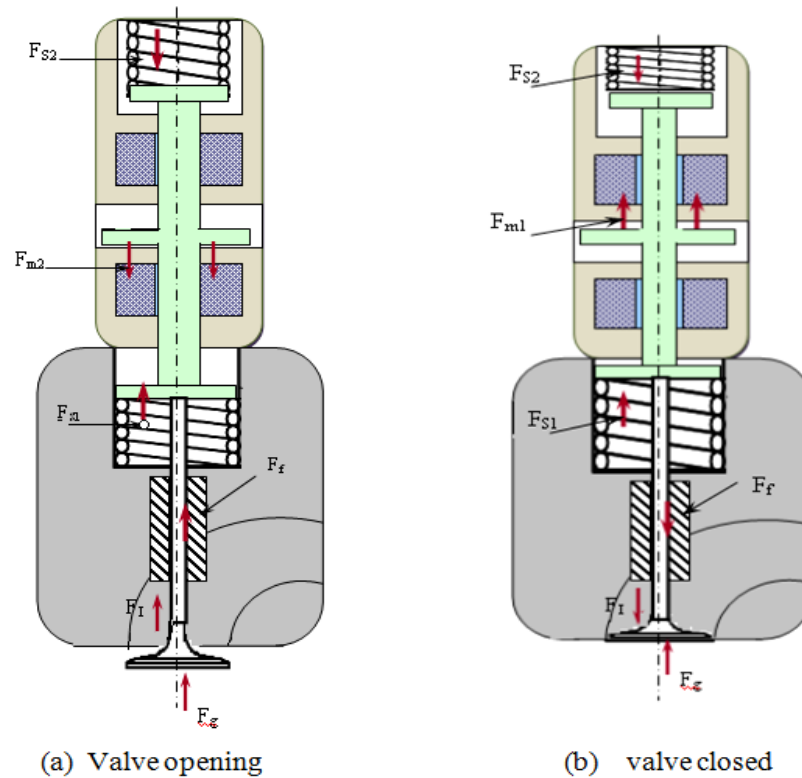


Figure 3. Forces acting on valve train actuator during operation and EMV system modeling

$$F_{m2} + F_{Su} - F_{SL} - F_f - F_{g1} = F_I \quad \text{for valve opening} \quad (12)$$

$$F_{m1} + F_{SL} - F_{Su} - F_f - F_{g2} = F_I \quad \text{for valve closing} \quad (13)$$

where F_{m1} , F_{m2} are the lower and upper magnetic forces. Any reciprocating mass of the electromechanical valve train (armature and valve) produces cyclic inertia forces, which can be evaluated from:

$$F_I = (m_v + m_a) * \frac{dv}{dt} \quad (14)$$

Where m_v is the valve mass, m_a the armature mass and $\frac{dv}{dt}$ is armature valve acceleration.

The valve spring force F_s is obtained simply by spring stiffness and multiplying the spring rate by the deflection of the spring from its installation and adding any preload, where $F_s = F_{in} + F_{con}$, $F_{in} = K \delta_o$ and $F_{con} = K * x_v$, then, $F_s = K [\delta_o + x_v]$.

The upper and lower spring forces:

$$F_{sL} = K_L [\delta_{o1} + x_v] \quad (15)$$

$$F_{su} = K_u [\delta_{o2} + x_a] \quad (16)$$

where F_{con} is the spring control force, F_{in} The spring initial support force, k_u , k_L are the upper and lower spring stiffness, δ_{o1} , δ_{o2} the upper and lower spring initial deflections, and x_v the valve lift.

The shearing resistance within the lubricant film in the clearance between the valve stem and its guide adds extra forces and to be considered in the analysis, under the sliding condition, the constant shear stress created equal to $\tau = \mu v / h$.

By Integration along the surface area of the stem, we get:

$$F_f = \tau [\pi d_g L_g] = \mu \frac{v}{h} [\mu d_g L_g] \tag{17}$$

At the instant, during the valve opening and closing, there is a difference in the pressure between the cylinder and the manifold which implies extra force on the system such as:

$$F_g = A_{fas} [\Delta p] = \frac{\pi}{4} d_{jac}^2 [p_g - p_v] \tag{18}$$

where F_g is the gas force due to gas pressure in the cylinder, F_f is the friction force due to hydrodynamic lubrication, γ is the oil viscosity, Table 1 tabulates the values of technical data for EMV.

Table 1 Technical data for EMV.

Parameters	Symbols	Units	Values
The valve mass	m_v	kg	0.16
The armature mass	m_a	kg	0.25
Supply voltage	V_{app}	voltage	24
Permeability in free space.	μ_o	H/m	$4\pi * 10^{-7}$
The resistance of both the wiring and magnetic coil	R	Ω	0.35
The valve guide diameter	d_g	m	$6 * 10^{-3}$
The valve guide length	L_g	m	$24 * 10^{-3}$
The valve and valve guide clearance	h	m	$0.5 * 10^{-3}$

3.3 EMV system model analysis

The mechanical part of the system, discussed in this paper, is similar to the one discussed in [14] except without having an apparent lash spring. However, it is still necessary to model the connection between the armature and the engine valve as a stiff spring since they are flexibly connected. The small signal linearization around some operating position and current gives:

$$dF_m = G_1 dx + G_2 di \tag{19}$$

where $G_2 = \frac{K_{ka} * i}{(K_{kb} + x)^2}$ and $G_1 = \frac{K_{ka} * i^2}{(K_b + x)^3}$.

The studied model of the valve actuator system is shown in Figure 4. The system has two masses, m_a (armature) and m_v (valve), the first mass is equivalent to the armature and the second mass is equivalent to the valve and spring. The valve actuator system connects to mass m_a through spring stiffness K_u and valve stem stiffness K_m and damper coeff. C_m between two masses and mass m_v is mounted by k_L, C_L . By summing forces and applying Newton's 2nd law;

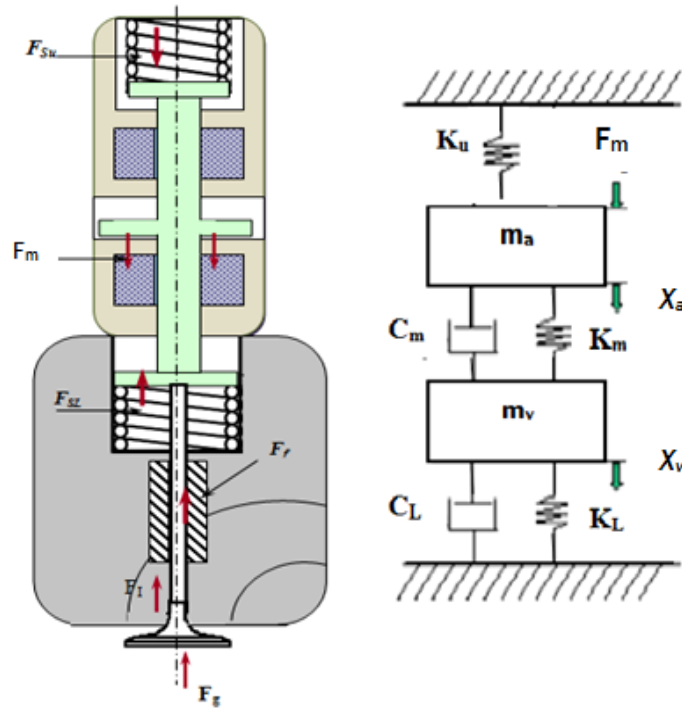


Figure 4. Forces acting on valve train actuator during operation and EMV system modeling

Equation of motion 2DOFS

$$m_a \ddot{x}_a - K_u x_a + C_m (\dot{x}_a - \dot{x}_v) + K_m (x_a - x_v) = F_m(t) \tag{20}$$

$$m_v \ddot{x}_v + K_L x_v + C_L \dot{x}_v - C_m (\dot{x}_a - \dot{x}_v) - K_m (x_a - x_v) = 0 \tag{21}$$

By reducing the equations to first order differential equations and formulate them in state space form:

$$\left. \begin{aligned} \dot{X} &= AX + Bu_{inp} \\ Y &= CX + Du_{inp} \\ x_1 &= x_a \quad x_2 = x_v \\ x_3 &= \dot{x}_a \quad x_4 = \dot{x}_v \\ \dot{x}_3 &= \frac{F_m}{m_a} + \frac{K_u}{m_a} x_1 - \frac{K_m}{m_a} (x_1 - x_2) - \frac{C_m}{m_a} (x_3 - x_4) \\ \dot{x}_4 &= \frac{K_m}{m_v} (x_1 - x_2) + \frac{C_m}{m_v} (x_3 - x_4) - \frac{K_L}{m_v} x_2 - \frac{C_L}{m_v} x_4 \end{aligned} \right\} \tag{22}$$

$$\begin{bmatrix} \dot{x}_1 \\ \dot{x}_2 \\ \dot{x}_3 \\ \dot{x}_4 \end{bmatrix} = \begin{bmatrix} 0 & 0 & 1 & 0 \\ 0 & 0 & 0 & 1 \\ \frac{(K_u - K_m)}{m_a} & \frac{K_m}{m_a} & \frac{-C_m}{m_a} & \frac{C_m}{m_a} \\ \frac{K_m}{m_v} & \frac{-(K_m + K_L)}{m_v} & \frac{C_m}{m_v} & \frac{-C_L - C_m}{m_v} \end{bmatrix} \begin{bmatrix} x_1 \\ x_2 \\ x_3 \\ x_4 \end{bmatrix} + \begin{bmatrix} 0 \\ 0 \\ 1 \\ 0 \end{bmatrix} F_m \quad (23)$$

Table 2 tabulates the values of main parameters of two-degree-of-freedom model.

Table 2 Main parameters of electromagnetic model data

Parameters	Symbols	Units	Values
The maximum valve displacement (lift)	x_v	m	$6 \cdot 10^{-3}$
The upper spring stiffness	K_u	KN/m	75
The lower spring stiffness	K_L	KN/m	75
The valve stem stiffness	K_m	KN/m	250
Viscous damping coefficient between armature and sleeve	C_m	N.s/m	60
Viscous damping coefficient between valve and guide.	C_L	N.s/m	60

Using Laplace operator (S) and the small-signal transfer functions from the magnetic force positions are:

$$m_a s^2 x_a - K_u x_a + K_m (x_a - x_v) + C_m s (x_a - x_v) = F_m(s) \quad (24)$$

$$m_v s^2 y_v + K_L x_v + C_L s x_v - K_m (x_a - x_v) - C_m s (x_a - x_v) = 0 \quad (25)$$

The transfer functions from the current to positions are;

$$\frac{dy_a}{di} = \frac{G_2 \{m_a s^2 + s C_m + (K_u + K_m)\}}{(m_a s^2 + s C_m + (K_u + K_m - G_1))(m_v s^2 + s(C_m + C_L) + (K_m + K_L)) - (s C_m + K_m)^2} \quad (26)$$

$$\frac{dy_v}{di} = \frac{G_2 \{s C_m + K_m\}}{(m_a s^2 + s C_m + (K_u + K_m - G_1))(m_v s^2 + s(C_m + C_L) + (K_m + K_L)) - (s C_m + K_m)^2} \quad (27)$$

The minimum valve travel speed in the EMVT depends on the natural frequency of the spring-mass system and is constant regardless of the engine speed. The natural frequency of oscillator is dependent on the oscillating mass and the spring stiffness. This limits the minimum opening duration of the valve. By increasing the spring stiffness and reducing the weight of the moving mass, the valve travel time can be reduced. But by increasing the spring stiffness, the electromagnetic force needs to be increased as well. By increasing the current the electromagnetic force can be increased as well. The electromagnetic force generated is proportional to the volume of the electromagnet. The design volume of the electromagnet is limited by the area in the cylinder head/block. Thus a compromise has to be made in the design and operation of an engine using EMVT system. These compromises are usually in the form of limiting volumetric efficiency of and maximum operating speed of the engine.

4. System control and stability

The system control of an electromagnetic valve (EMV) is described. This is using electromagnetic force to open and close the valve and a controller regulates the motion by control the variation of current duration with time. But, however the sensitivity of the transient motion to disturbances depends much on the system stability.

The system has to be stabilized with a tuned PID controller before the system identification test could be executed. The PID controller works in a closed-loop system using the schematic in Figures 5 and 6. The variable e represents the tracking error, the sent to the PID controller and the controller computes both the derivative and the difference between the desired input value R and the actual output Y . This error signal e will the signal u just past the controller is now equal to the proportional gain K_p times the magnitude of the error plus the integral gain K_i times the integral of the error plus the derivative gain K_d times the derivative of the error.

$$u = K_p e + K_i \int e dt + K_d \frac{de}{dt} \tag{28}$$

Adjust each of K_p , K_i and K_d until the desired overall response is obtained, by choosing the values of $K_p=38020$, $K_i=520$, and $K_d=7.85$

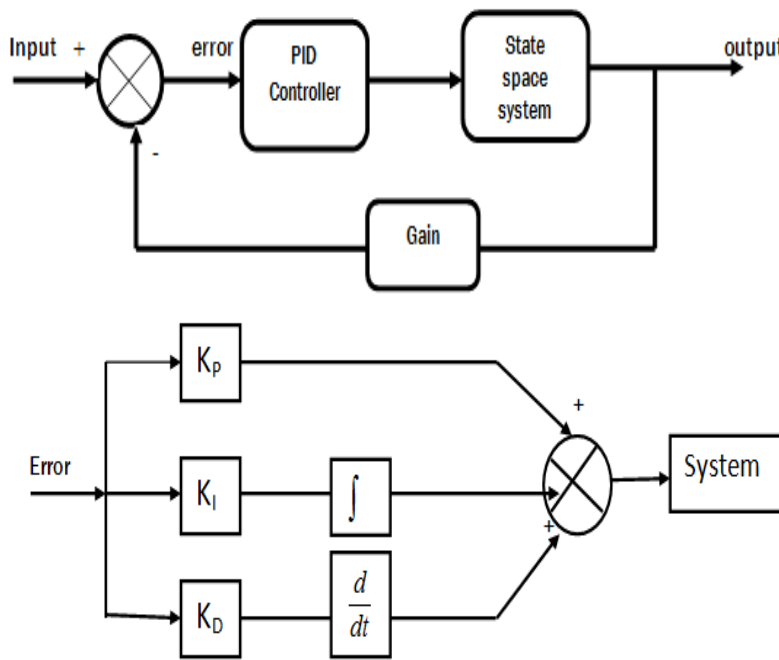


Figure 5. PID Controller without current applied

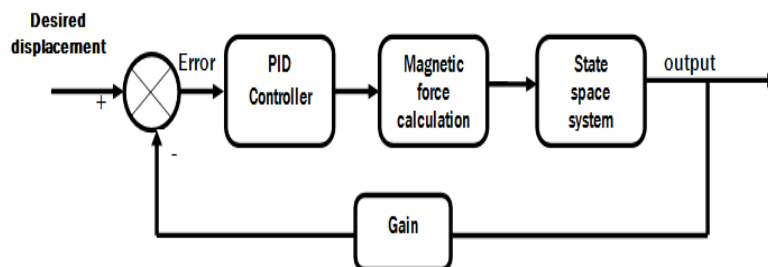


Figure 6. PID controller with current applied

5. LQR Optimal control dDesign

Linear-quadratic regulator design (LQR) for continuous-time systems is used to calculate the optimal gain matrix K such that the state-feedback law $\dot{x} = Ax + Bu_{inp}$ with outputs $Y = cx$.

This model has two states, the armature position and velocity. The position can be directly measured, and the velocity can be estimated with the differentiation of position measurements. An LQ optimal controller is designed for stabilizing the augmented plant. The cost function that needs to be minimized is $u = -Kx$ minimizes the following cost function:

$$J = \int_0^{\infty} [x^T c^T q c x + u^T R u] dt \quad (29)$$

where

x = the system state variables

u_{inp} = the control signal

Y = system outputs

c = the output matrix

R and q are the weighting parameters. The problem can be solved by introducing the following Riccati equation:

$$SA + A^T S - (SR + N)R^{-1}(B^T S + N^T) + c^T qc = 0 \quad (30)$$

Where

S = Riccati matrix

A = EMV characteristic matrix

B = the input matrix.

Matlab program is used to calculate the gain matrix K using the following form $[K, S, E] = lqr(A, B, Q, R, N)$.

Note that is derived from by limitations the problem data must satisfy, under the following conditions:

- The pair matrix A and B are stabilizable.
- $R > 0$
- $c^T qc - NR^{-1}N^T \geq 0$
- $A - BR^{-1}N^T \geq 0$

Chooses the values of weighting parameters by return repetition to the minimize value of performance index. The values of weighting parameters are $R=2.18*10^{-7}$ and $q=1.18$.

The values result of feedback gains are $K = [52.3*10^2 \quad 6.38*10^3 \quad 874.2 \quad 8.29*10^2]$, the control input signal is: $u(t) = 52.3*10^2 X_1 + 6.38*10^3 X_2 + 874.2 X_3 + 8.29*10^2 X_4$, and the closed-loop eigenvalues the system is stable :

$$E = \begin{bmatrix} -0.2372 & +3.4743 & i \\ -0.2372 & -3.4743 & i \\ -2.126 & +11.293 & i \\ -2.126 & -11.293 & i \end{bmatrix} * 10^2$$

6. Results and discussion

General requirements of valve lift, it is highly desirable to achieve a maximum valve lift as soon as possible after the initiation of valve opening. The reason is that with a fast valve opening sequence, the flow over the valve will be less restricted during a greater part of the valve lift duration and result in higher volumetric efficiency. Figure 7 illustrates an optimal valve lift profile with an infinitely fast valve opening and valve closing. However, such a valve lift profile would be impossible to implement in reality, since an instantaneous valve opening and closing would mean infinite acceleration of the valve which would be much too severe for any valve train to endure. Also, the valve has to slow down as it approaches the seat in order to prevent the valve from hitting the seat with loud noises, and worn and

broken parts as a result. The required of valve designed to have approximately the same valve opening and closing characteristics for wide ranges of engine speeds. They provide a smooth and continuous change of the valve lift is shown in Figure 8.

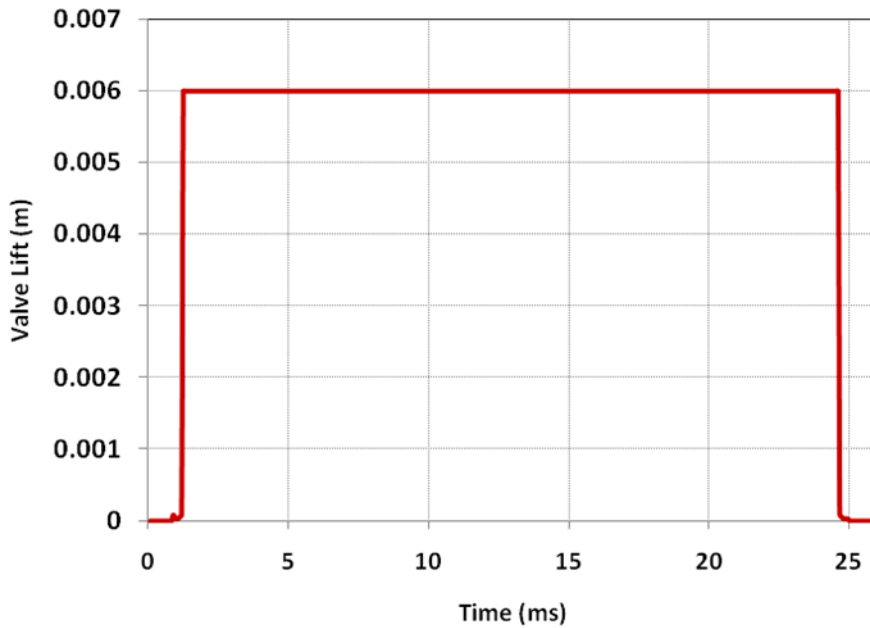


Figure 7 The optimal valve lift requirement

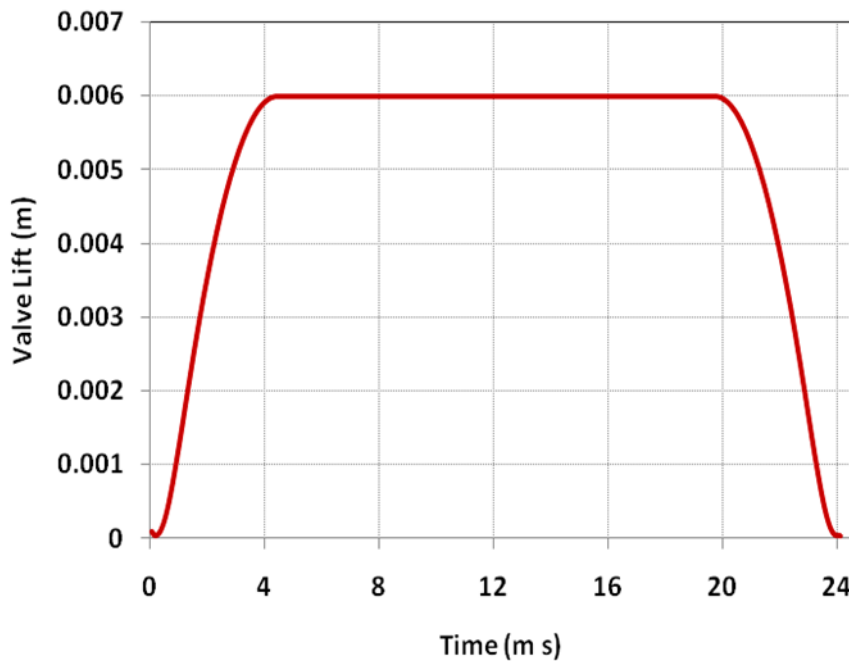


Figure 8 The smooth valve lift requirement

Figure 9 illustrates the nonlinear B-H curve. Figures 10 and 11 depict the influence of armature distance on the magnetic force, current of the magnetic coil and spring force. Figure 12 show the current and power of EMV with different time for upper coil excited, with the upper and lower coils excited the with different lift and different time (crank angles) can be calculate the armature displacement is presented in Figure 13.

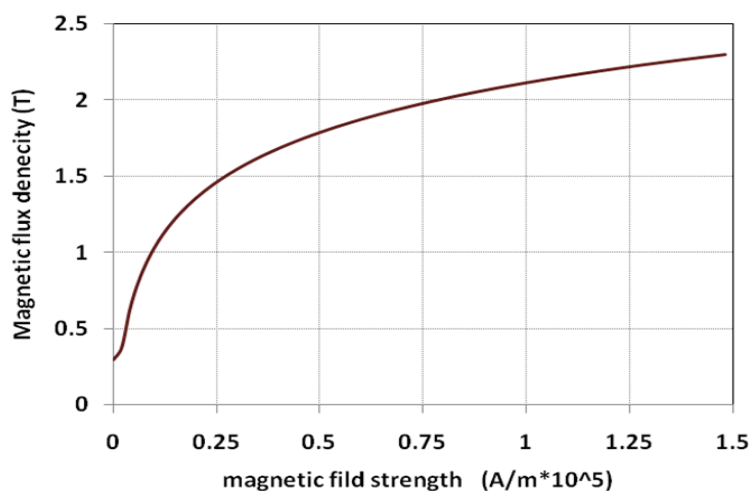


Figure 9. B-H curve

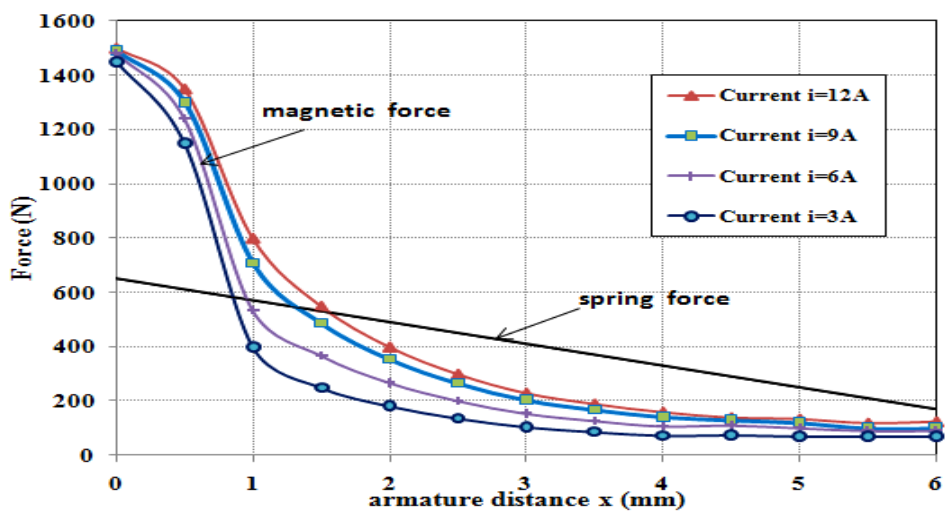


Figure 10. Relation between magnetic force with armature distance for varying current

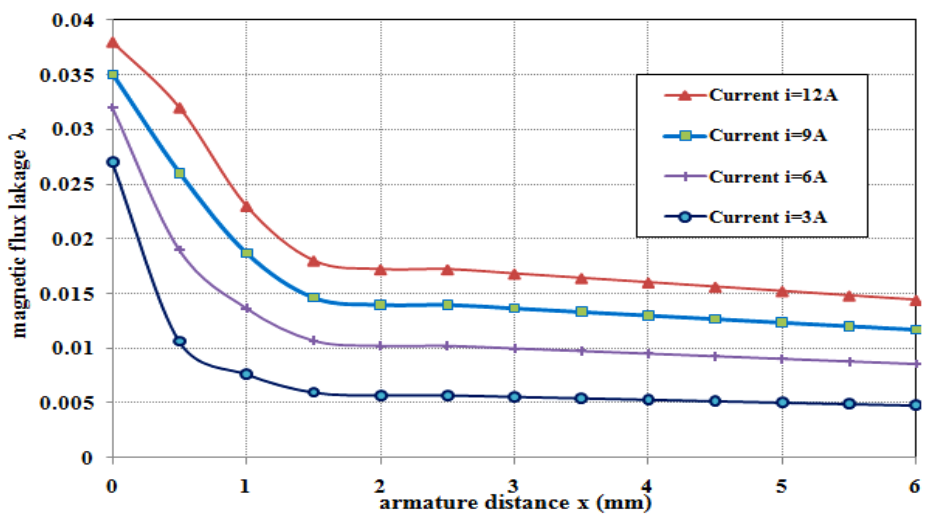


Figure 11. Relation between magnetic flux with armature distance for varying current

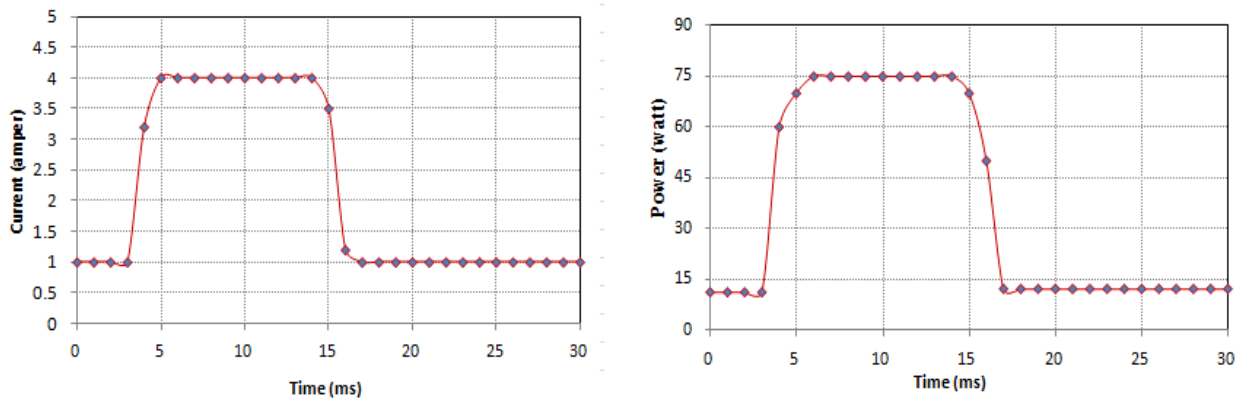
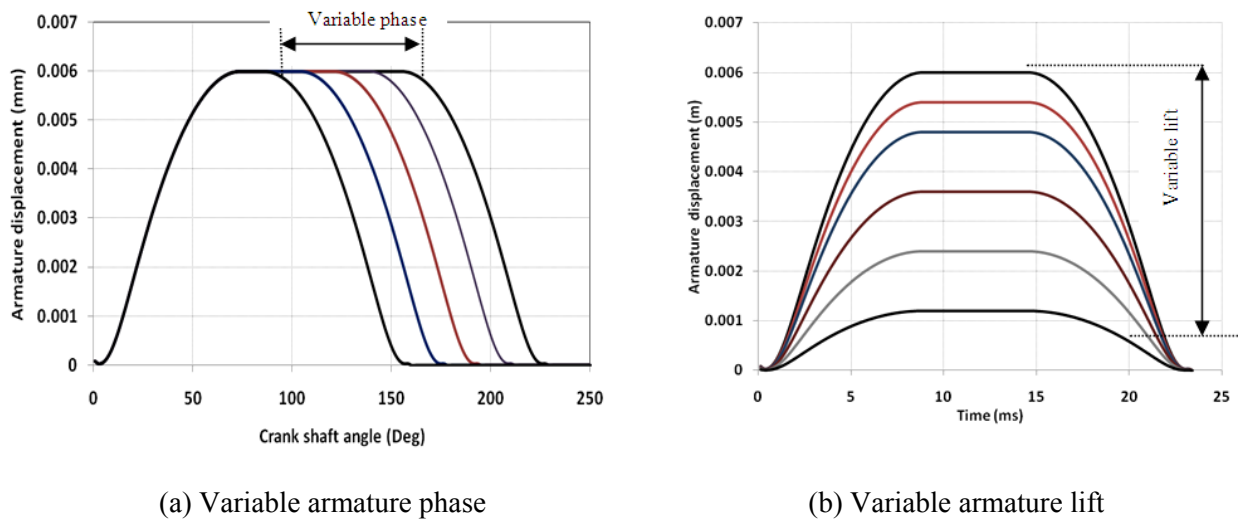


Figure 12. EMV current and power with operating upper coil excited



(a) Variable armature phase

(b) Variable armature lift

Figure 13. Armature displacement

Figure 14 illustrates the system response in time-domain and the analysis is generated with zero current, and Figure 15 illustrates the response of the in frequency-domain.

Figure 16 depicts the EMV response with the controller. The effects of each of controllers K_p , K_D , and K_I on a closed-loop system are improved the rise time is reduced by 4.5 ms. the overshoot is improved and the steady-state error of the system is eliminated.

The valve and armature distance are shown in Figure 17 with the upper and lower magnetic coils are operated. The feedback controller is to reduce the sensitivity of the system to disturbance and maintain valve motion along the given reference trajectory and the valve and armature acceleration illustrates in Figure 18. The armature energy shown in Figure 19. Because of the current values, a non-linear behavior of the material has been considered, by the valve mass, armature mass and system acceleration can be calculate the inertia force, The influence of EMVT comparison between forces at 6000 rpm are illustrated in Figure 20, the magnetic force overcome the inertia force, friction force and spring force with good operation.

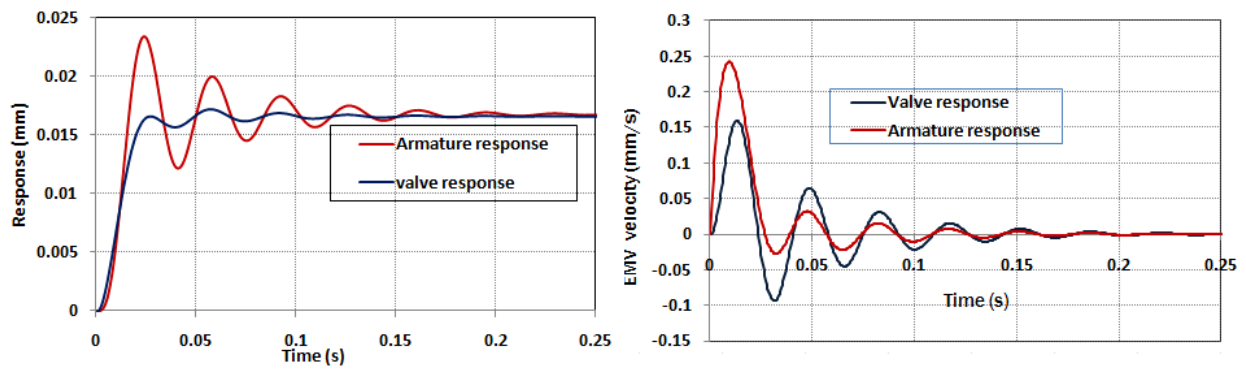


Figure 14. EMV Free responses with no current

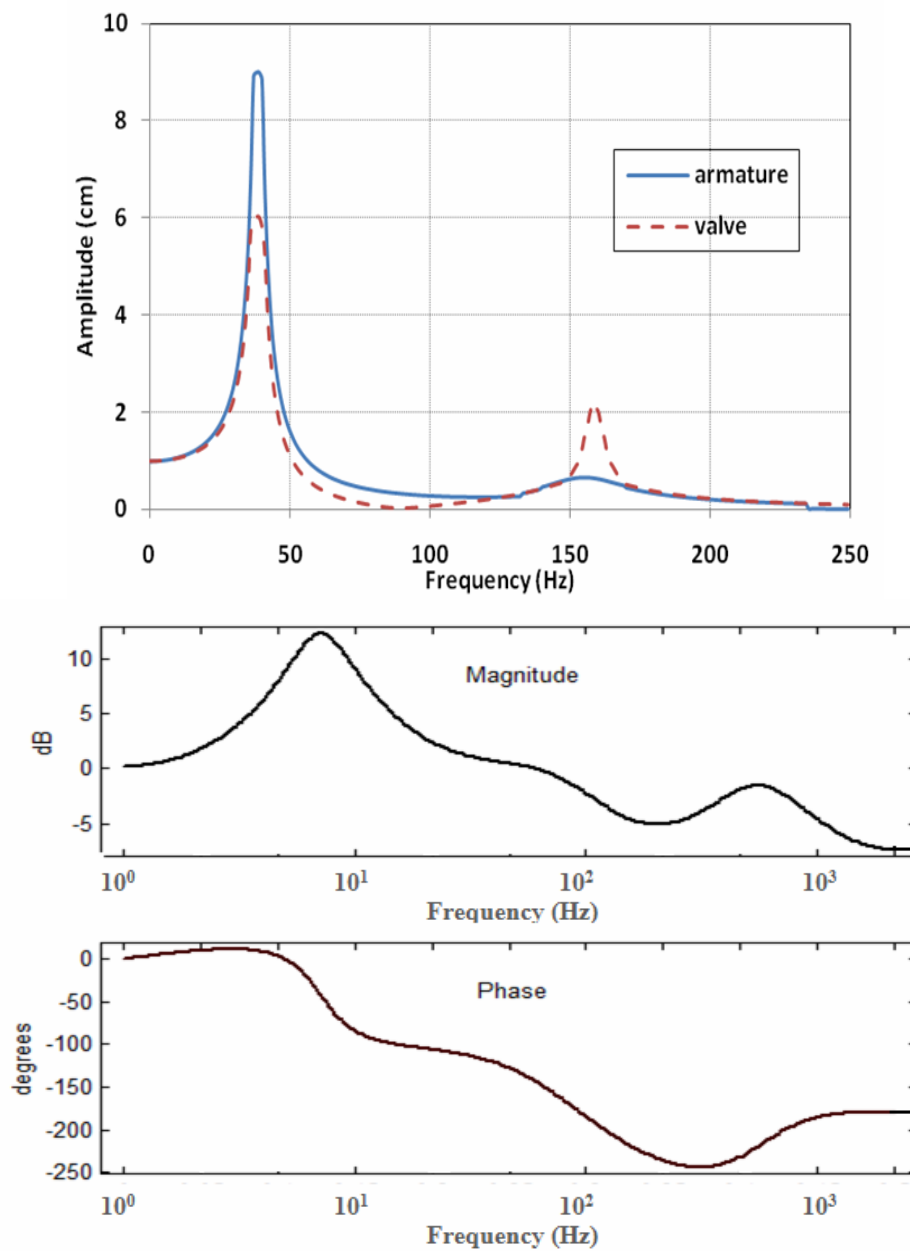


Figure 15. EMV Frequency responses

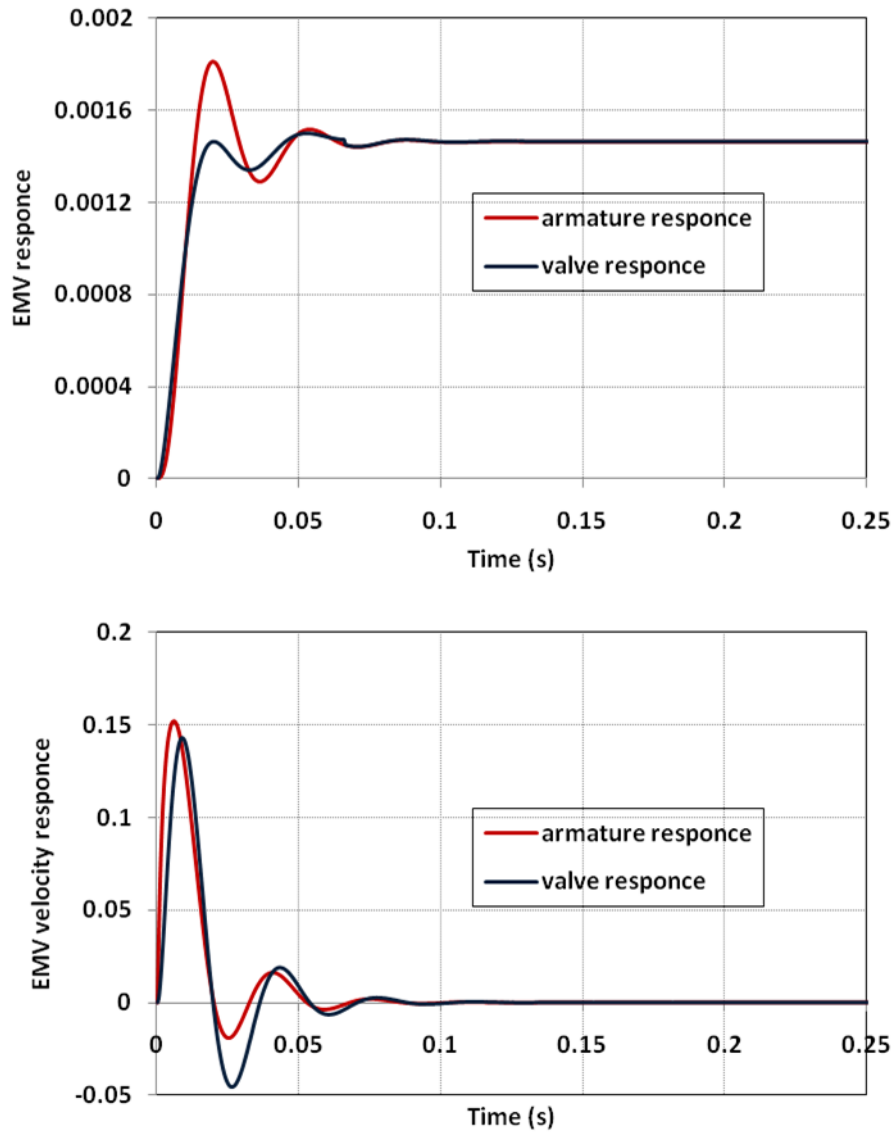


Figure 16. EMV Free responses with PID controller at no current

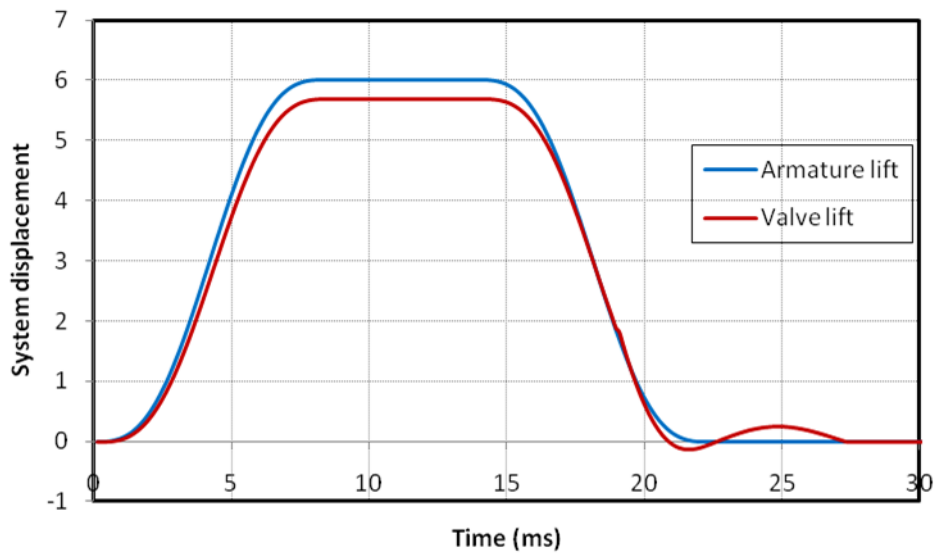


Figure 17. Valve lift and armature lift, by upper and lower coil currents

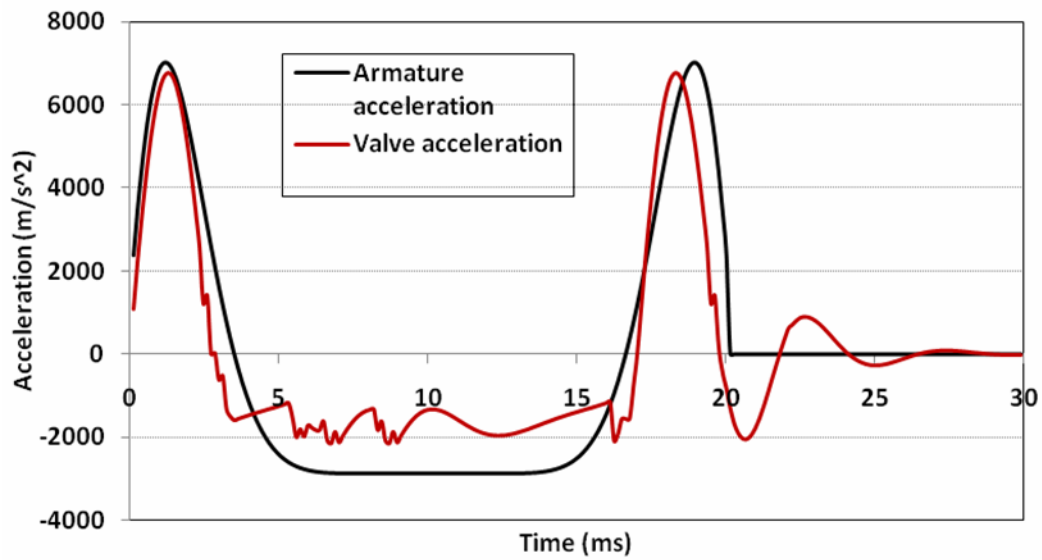


Figure 18. Valve and armature acceleration

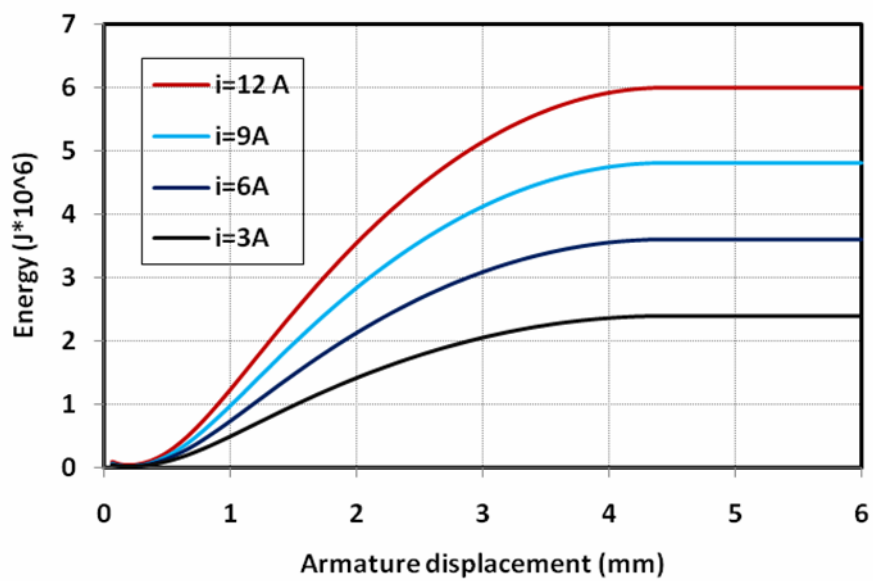
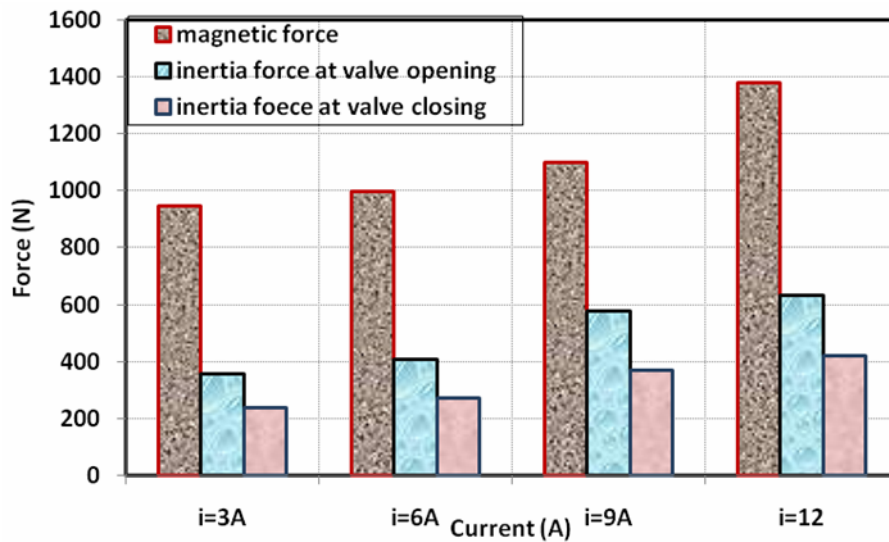
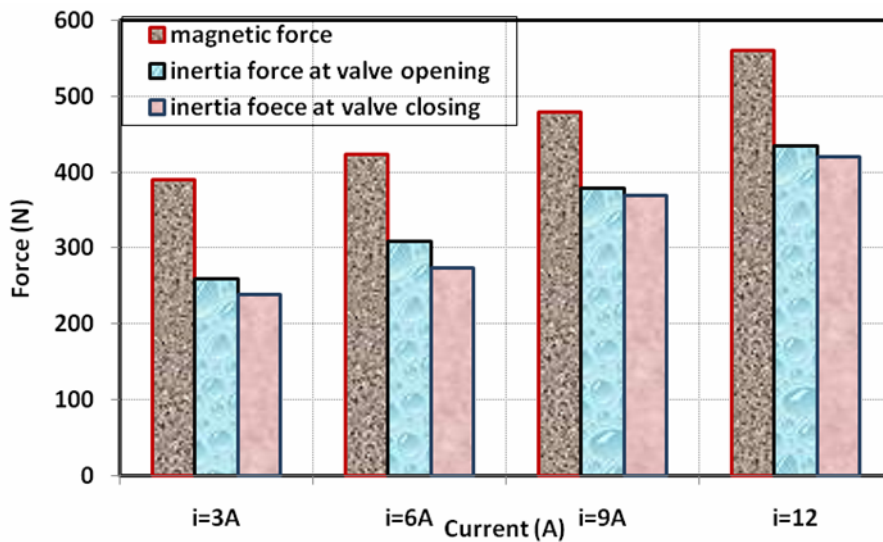


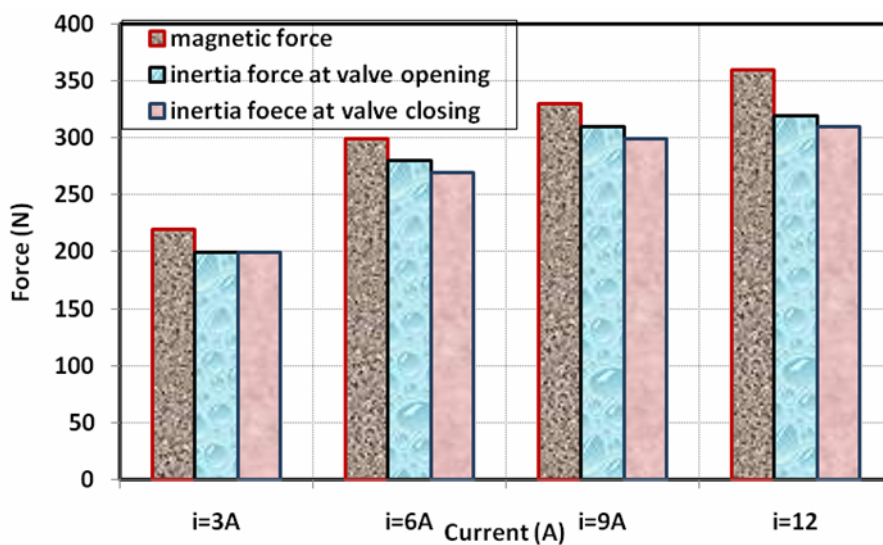
Figure 19. The armature energy for upper coil



(a) Valve lift 0.5 mm



(b) Valve lift 3 mm



(c) Valve lift 6 mm

Figure 20. RMS of forces acting on valve with different current

7. Conclusion

In this paper, we present the design and simulation modeling of a one type of camless engine. The results confirm that the proposed EMV achieves variable valve motion while maintaining the essential characteristics of internal combustion engine valve drives. A relatively simple and accurate EMV model is developed for control development and evaluation. The simulation model takes eddy current effects, magnetic saturation, power electronics and filter algorithms into account to improve transient behavior approximations. The identified parameters were used to develop a linear EMV actuator model. A closed loop controller was designed for stabilizing the actuator by using PID control. A position feedback closed-loop controller was designed and implemented in order to reduce the valve landing velocity from 0.52 m/s to 0.23 m/s with consistent transition time of 3.42 ms. The results obtained with the proposed model are in good agreement with the optimal criteria; some analyses have been performed for fixed coils, varying the armature geometry to minimize the power consumption.

a	Armature acceleration.
C_m, C_L	Model viscous damping coefficient.
d_{fac}	Valve face diameter.
d_g	Valve guide diameter.
$EMVA$	Electromechanical valve actuator.
F_f	Friction force due to hydrodynamic lubrication between valve stem and guide.
F_{g1}, F_{g2}	Gas force due to pressure in the cylinder at the instant the valve opens and closes.
F_i	Armature and valve inertia force.
F_m	Magnetic force generated by the magnetic coil.
F_{m1}, F_{m2}	Magnetic force generated by the upper and lower magnetic coil.
F_{sL}, F_{sU}	Lower and upper control spring force.
h	The valve and valve guide clearance.
i	The current in the magnetic coil.
K_a, K_b	The constant factor.
K_m	The valve stem stiffness.
$K_p, K_D, \text{ and } K_I$	Gains of PID controller closed-loop.
K_u, K_L	Upper and lower spring stiffness.
L	Inductance.
L_g	Valve guide length.
LQR	Linear-quadratic regulator.
N	Number of winding turns.
P_g	The pressure in the cylinder at instant the valve opens or closes.
P_v	The pressure in the manifold.
R	Resistance of both the wiring and magnetic coil.
u_{inp}	The control signal.
v	Armature velocity.
V_{app}	The voltage applied to the magnetic coil.
x_a	Armature displacement.
Y	System model outputs.
Z_1	Back EMF generated by the armature motion.
Z_2	Inductance of the magnetic coil.
λ	Nonlinearities of flux linkage.
λ_s	Maximum saturated flux.
Φ_l	Leakage flux.
Φ_m	Magnetizing flux.
γ	The oil viscosity.

References

- [1] K. Jinho and C. Junghwan. "A new electromagnetic linear actuator for quick latching" IEEE Transactions on Magnetics, (2007).

- [2] T. A. Parlikar, M. D. Seeman, W. S. Chang, D. J. Perreault "Design and Experimental Implementation of an Electromagnetic Engine Valve Drive" IEEE/ASME Vol. 10, No. 5, 2005
- [3] Riheb Wislat, Helmut Haase "Static and Dynamic Simulation of an Electromagnetic Valve Actuator Using COMSOL Multiphysics" COMSOL Conference 2009 Milan.
- [4] M. Pischinger, W. Salber, F. V. D. Staay, H. Baumgarten and H. Kemper "Low Fuel Consumption and Low Emissions Electromechanical Valve Train in Vehicle Operation" FISITA World Automotive Congress,(2000).
- [5] Jieng-Jang Liu Yee-Pien Yang, Jia-Hong "Electromechanical Valve Actuator with Hybrid MMF for Camless Engine" World Congress the International Federation of Automatic Control, 2008 IFAC.
- [6] Katherine S. Peterson and Anna G. Stefanopoulou "Rendering the Electromechanical Valve Actuator Globally Asymptotically Stable" Proceedings of the 42nd IEEE, Conference on Decision and Control, Maui, Hawaii USA, December 2003.
- [7] Y. H.Qiuz, W., M. D.Seemanz, T., D. and J. G.Kassakian "Design and Experimental Evaluation of An Electromechanical Engine Valve Drive: 35th Annual IEEE Power Electronics Specialists Conference, (2004).
- [8] J. W. G. Turner, M. D. Bassett, R. J. Pearson, G. Pitcher and K. J. Douglas" New Operating Strategies Afforded by Fully Variable Valve Trains", SAE paper, SAE World Congress, Michigan ,(2004).
- [9] KatherineS.Peterson, Anna.G. Stefanopoulou, Yan Wang, Tom Megli "Virtual Lash Adjuster for an electromechanical valve actuator Through Iterative Learning control" IMECE2003-41270, 2003 ASME International Mechanical Engineering Congress.
- [10] S H Khan, M Cai, K T V Grattan, K Kajan, M Honeywood and S Mills "Design and investigation of high-speed, large-force and long life time electromagnetic actuators by finite element modeling" Journal of Physics: Conference Series 15 300–305,(2005).
- [11] S-H Park1, J Lee, J Yoo, D Kim and K Park, "Effects of design and operating parameters on the static and dynamic performance of an electromagnetic valve actuator" Proc. Instn. Mech. Engineers Vol. 217 Part D: J. Automobile Engineering, pg. 193-201. (2003).
- [12] Y. Wang, T. Megli, M. Haghgooe, K.S. Peterson and A.G "Modeling and Control of Electromechanical Valve Actuator "SAE 2002-01-1106, (2002).
- [13] Chun Tai, Tsu-Chin Tsao "Control of an Electromechanical Camless Valve Actuator" American Control Conference 2002 AACC May 8-10, 2002.
- [14] Brader S, "Development of a Piezoelectric Controlled Hydraulic Actuator for a Camless Engine "Thesis 2001, College of engineering and Information Technology, University of South Carolina.